Empa
Überlandstrasse 129
CH-8600 Dübendorf
T +41 58 765 11 11
F +41 58 765 69 93
www.empa.ch

Empa
Materials Science and Technology

Herr Franz Kuster
Bundesamt für Umwelt BAFU
Sektion Eisenbahnlärm
Monbijoustrasse 40
3003 Bern

Preliminary experimental study of the influence of loose rail clamps on track dynamics

Research report: Empa-Nr. 5211.02162

Your order of: 23. March 2022

Number of pages: 24

Contents

Dübendorf, 20. April 2022
Project leader:

Bart Van Damme

Digitally signed by Bart Van Damme
Date: 2022.07.11 10:55:43 +02'00'

Dr. Bart Van Damme

Laboratory for Acoustics / Noise Control
Lab leader:

Jean-Marc Wunderli

Digital unterschrieben von Jean-Marc Wunderli
Datum: 2022.07.11 10:52:06 +02'00'

Dr. Jean Marc Wunderli

The report and documentation are archived for 10 years

Imprint

Customer
Fredy Fischer, Franz Kuster
Bundesamt für Umwelt (BAFU),
Robert Attinger, Christoph Dürig
Bundesamt für Verkehr (BAV)

Author/Contractor

Bart Van Damme
Empa, Überlandstrasse 129, 8600 Dübendorf, Tel. +41 58 765 41 10

Remark: This study was commissioned by the Federal Office for Environment. The contractor alone is responsible for the content.

Zusammenfassung

Bei den Lärmemissionen der Eisenbahnen strahlen insbesondere der Bahnoberbau und das Fahrzeug (speziell das Rad) Schall ab. Im vorliegenden Projekten geht es nur um den Bahnoberbau. In einem Forschungsprojekt des BAFU und des KPZ Fahrbahn AG von 2021 hat sich gezeigt, dass bei einem regulären Bahnoberbau bis rund 15% der Schienenbefestigungen nicht korrekt angezogen sind. Korrekt angezogen heisst in diesem Fall, dass der Luftspalt zwischen der Mittelschleife der Spannklemme und der Winkelführungsplatte maximal 0.5 mm beträgt. Dies kann zu Inhomogenitäten im Gleis hinsichtlich der Steifigkeit führen.
Im vorliegenden Forschungsprojekt werden die Auswirkungen von nicht korrekt angezogenen Schienenbefestigungen untersucht. Alle Untersuchungen fanden auf dem Testgleis der TU München statt. Dieses besteht aus 18 Schwellen mit Befestigungen SKL14 (System W14) in einem Schotterbett. Die untersuchte Auswirkungen von losen Schienenbefestigungen sind

- veränderte Beschleunigungen der Schienen am Ort der Krafteinwirkung (point mobility)
- veränderte Track Decay Rate (vertikal)
- veränderte Schwingungsübertragung von der Schiene in den Untergrund
- veränderte Lärmabstrahlung des Oberbaus

Diese Effekte wurden für drei unterschiedliche Zwischenlagen (ZWs) gemessen: harte EVA ZWs (üblich bei SBB), weiche Vossloh ZWs (ausnahmsweise bei SBB) und ZWs mit hoher Dämpfung und mittlere Steifigkeit (hergestellt von Semperit im Rahmen eines Forschungsprojektes).
Weil vorherige Messungen gezeigt haben, dass es nur bei ganz loosen Klemmen messbare Unterschiede in der Lärmabstrahlung gibt, werden nur die Situationen betrachtet bei welchen die Spannklemmen entweder komplett angedreht oder komplett lose sind. Dabei wurden sieben Situationen untersucht:

Setup 1 Alle Klemmen sind angezogen

Setup 2 Beide Klemmen der Schwelle 9 sind lose

Setup 3 Beide Klemmen der Schwellen 8–9–10 sind lose

Setup 4 Beide Klemmen der Schwellen 7–8–9–10–11 sind lose

Setup 5 Beide Klemmen der Schwellen 6–7–8–9–10–11–12 sind lose

Setup 6 Beide Klemmen der Schwellen 2–5–6–9–10–13–15 sind lose

Setup 7 Alle Klemmen sind wieder (manuell) angezogen

Der Extremfall mit 15% losen Klemmen stimmt also mit Setup 3 überein, weil nur Messungen an einer Schiene durchgeführt werden. Setup 4–6 haben bis 1/3 lose Schwellen, um jeweilige Trends besser erkennen zu können. Die Erkenntnisse sind wie folgt:

- Die Punktmobilitäten ändern sich unterschiedlich nach Frequenz. Im Bereich 200-800 Hz nimmt die Mobilität zu wenn es mehr lose Klemmen gibt, um die 1000 Hz (pin-pin mode) nimmt sie ab und ab 1500 Hz bleibt die Mobilität gleich. Der Effekt wird kleiner bei weicheren ZWs.
- Die vertikale TDR nimmt bis 2000 Hz deutlich ab, wenn mehrere Klemmen schlecht angezogen sind, dies allerdings deutlich weniger bei weicheren ZWs. Die festgelegte Grenzwerte werden aber meistens nicht überschritten, ausser in extremen Fällen. Es braucht sieben lose Klemmen nebeneinander für harte ZWs, um die untere Grenzwert zu überschreiten. Im Frequenzbereich 300-600 Hz erreichen sehr weiche ZWs die vorgeschriebenen Grenzwerte nie.
- Die Schwingungsübertragung in den Boden ändert sich nicht messbar. Nur im Fall der steifen ZWs könnte bei ganz tiefen Frequenzen eine leichte Verringerung der Energieübertragung auftreten.
- Die Schalleistungspegel und Schalldruckpegel ändern sich geringfügig wenn harte ZWs gebraucht werden. Bei einzelnen Frequenzen nimmt die Schalleistung zu, bei anderen ab. Eine quantitative Bestimmung war wegen der experimentellen Bedingungen (Reflektionen im Raum und Rauschen wegen schlechten Wetters) nicht möglich. Bei weicheren ZWs sind die gemessenen Unterschiede noch kleiner. Näher zur Quelle gibt es für alle ZWs eine kleine Zunahme der Schalldruckpegel im Bereich 1000-3000 Hz. Dies könnte ein Effekt der kleineren TDR sein.

Die Messungen am Testgleis zeigen, dass 15% lose Klemmen die massgeblichen akustischen und dynamischen Werte so wenig ändern, dass sie in der Wahrnehmung vernachlässigbar sind. Die gemessene Änderungen sind geringer wenn die ZWs weicher oder aus einem dämpfenden Material hergestellt sind.

1 Assignment

By contract 1337000623 dated 4 April 2022, the Federal Office for Environment commissioned an experimental study of the presence of loose rail clamps on the dynamic and acoustic behaviour of a railway superstructure. Since on-track inspections show that up to 15% of the fasteners are insufficiently tightened [1], the question arises if this leads to increased noise or vibration transmission. An investigation of a 3-sleeper lab setup showed that there is a measurable effect on the rail dynamics, but a small effect on the acoustic radiation, which is measurable only in case all clamps are fully loosened [2].
This study investigates the dynamic effect of fully loosened clamps on the following railway superstructure properties:

1. Point mobility
2. Track decay rate
3. Vibration transmission
4. Sound radiation

The measurements were performed with three distinct types of rail pads: standard hard EVA pads (600kN/mm) and soft PU pads (Vossloh, 100kN/mm) used by SBB, and an experimental high-damping railpad (Semperit, 300kN/mm) developed in collaboration by EPFL, HEIG, and Empa.

2 Experimental setup

2.1 General information

The measurements were performed on 25–27 april 2022 by Dr. Bart Van Damme, Dr. Andrea Bergamini and Mr. Linus Taenzer. The TUM responsible was Mrs. Veronika Kollmeier.
The measurements were performed using a 32-channel National Instruments measurement system consisting of a chassis type PXIE-1073, containing two measurement cards PXIe-4499 and a signal generator PXI-5402.

2.2 Test track

The measurements were performed on the test track owned by TU München, Lehrstuhl und Prüfamt für Verkehrswegebau (Franz-Langinger-Straße 10, 81245 München). It is a ballasted track with 18 concrete sleepers similar to the type B91. The rail is fastened by a standard Vossloh fastening system (clamp SKL14, angle plate Wfp 14K, bolt Ss35). The ballast rests on a concrete floor. Details of the test track are shown in Fig. 1.
All dynamic properties of the track are measured in seven situations (called setup 1 – 7). They are defined as follows:

Setup 1 All clamps are tightened by an electrical screwdriver up to maximum torque. The torque is not measured.

Setup 2 The two bolts of sleeper 9 are loosened completely

Setup 3 The two bolts of sleepers 8–9–10 are loosened completely

Setup 4 The two bolts of sleepers 7–8–9–10-11 are loosened completely

Setup 5 The two bolts of sleepers 6–7–8–9–10–11–12 are loosened completely

Setup 6 The two bolts of sleepers 2–5–6–9–10–13–15 are loosened completely

Setup 7 All clamps are tightened by a manual wrench up to maximum torque. The torque is not measured.

These seven situations were established with three types of railpads representing a wide range of situations. The first type is the standard hard EVA railpad (SBB Zw661 - 600 kN/mm), the second a very soft PU railpad (SBB Zw 700a, 100 kN/mm), the third a novel pad with high viscoelastic damping and intermediate stiffness (Semperit, 300 kN/mm).

Figure 1: Images of the full track, and detail of the clamping system (left). The right image shows the outer sleeper which is not fully embedded in the ballast.

2.3 Measurement of the point mobility

The point mobility is defined as the ratio between an input force and the resulting rail acceleration, both measured in the same point. The force was generated by an instrumented hammer (PCB086B03) hitting the rail vertically on the top. The acceleration was measured by an accelerometer (PCB352C68). The time response of ten impacts was measured to allow sufficient averaging. A 0.25 s signal was measured with a sampling rate of 100 kHz.
The point mobility was measured mid-span between sleepers 9 and 10, so for Setup 2 – 6 in the vicinity of a loose clamp.

2.4 Measurement of the Track Decay Rate

Measuring TDR on a short track has particular practical difficulties and is only an approximation of the true value on an infinite track. The main reasons are (i) the presence of reflected waves in the short track section and (ii) the assumption that measurements can be done up to a distance where all signals have completely decayed. We propose not to use the standard formula from the norm EN 15461:2008 since this explicitly assumes total decay of the waves, which cannot be achieved on an 18m-long track. However, the exponential decay can also be derived by fitting the amplitude decay as a function of distance. This method was proposed in [4].
For faster measurement, the rail was excited by one source (mid-span between sleepers 4 and 5), and its response was simultaneously measured by 18 accelerometers (B&K 4513, sensitivity 450 mV/g). The source was a shaker (TIRA TV 51120) applying a vertical force on the rail, measured by a force sensor PCB 208C02 with a sensitivity of 10 mV/N. The excitation signal was a linear sweep ranging from 50 Hz to 4000 Hz in 5 s, with a sampling rate of 50 kHz. The first accelerometer was positioned directly next to the shaker, the second at a distance of 0.15 m, and the consequent sensors were spaced with an equal distance of 0.3 m. With this setup, the wave propagation is measured over a distance of 4.95 m, avoiding the free edges of the rails. The positions were chosen so that none of the accelerometers were placed directly on top of a sleeper as shown in Fig. 2. The practical setup is shown in Fig. 4.

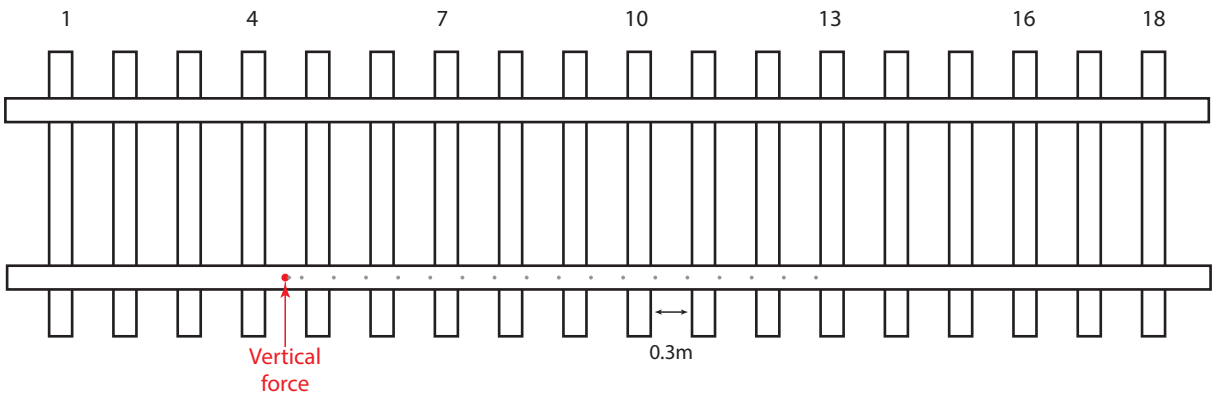

Figure 2: Schematic representation of the position of the force excitation (red) and the 18 accelerometers (grey) for the TDR measurement.

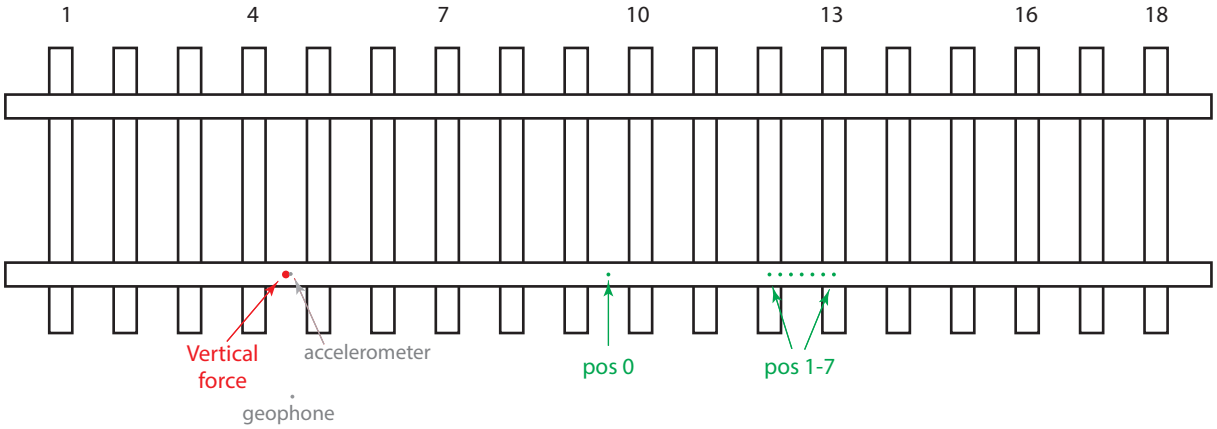

Figure 3: Schematic representation of the position of the force excitation (red), the reference rail accelerometer and geophone (grey), and the 8 positions for the microphone array (green).

2.5 Measurement of rail - floor vibration transmission

The vibration transmission from the rail to the concrete subgrade is measured using two accelerometers. One reference accelerometer is placed next to the force excitation using the same setup and excitation signal as in Section 2.4. The ground vibration is measured using a geophone PCB 393B31 with a 10 V/g sensitivity placed right next to the ballast bed, at the same horizontal location as the reference accelerometer. The situation is shown in Fig. 3.

2.6 Measurement of acoustic radiation

The sound pressure level is measured using an array of 7 microphones placed on a semicircle with radius 1 m around the rail. The rail is excited by a shaker in the same way as described in Section 2.4. The microphone array is moved in 8 positions. Position 0 is midspan between sleeper 9 and 10, close to the clamp that is loosened in Setup 2–6. Positions 1–7 span the entire sleeper section between sleepers 12 and 13, moving the array 10 cm for each next position. The microphone array positioned are shown in green in Fig. 3. The microphone array itself is shown in Fig. 4.

3 Point mobility

3.1 Data analysis

The point mobility is given as a spectrum, showing the ratio between the vertical acceleration of the rail and the input force generated by the instrumented hammer. The transfer function is calculated in Matlab R2020b using the command `tfestimate`. Alternatively, the power spectra are calculated in third-octave bands using the command `poctave`. In the following sections, all results are shown as power spectra, with units $(\mathrm{m/s^2/N})^2$.

Figure 4: Photos of the experimental setup. Top left: shaker connected to the rail, and four first accelerometers. Bottom left: entire test section with shaker in the background and microphone array in position 5. Right: close up of the microphone array showing the orientation of the microphones. The last three accelerometers are also visible.

3.2 SBB hard pads

The mobilty is shown in Fig. 5 for setup 1–6, 1 being all clamps tightened, and increasing the number of loose clamps up to setup 5. Setup 6 has the clamps on 7 random sleepers loosened.
We can distinguish three frequency regimes. Between 200 an 700 Hz, the regime mainly governed by the sleeper dynamics, the mobility increases when more clamps are loosened. At the mobility peak around 1000 Hz, the first vertical pin-pin vibration mode, the mobility decreases when the clamps are loosened. Starting at 1500 Hz, the typical range for rail dynamics, the clamps do not seem to play an important role as the mobility does not change.
We would like to point out that Setup 6, having the clamps loosened on 7 sleepers scattered over the length of the track, the effect on the mobility can be measured but it follows the curve of Setup 3 (clamps loosened on 3 consecutive sleepers).
In absolute numbers, the mobility power increases with a factor 5 at 400 Hz when the clamps of 7 consecutive sleepers are loosened. The mobility power is reduced by a factor 2.7 at the pin-pin frequency 1000 Hz in that case.

3.3 SBB soft pads

The mobility is shown in Fig. 7 for setup 1–6, 1 being all clamps tightened, and increasing the number of loose clamps up to setup 5. Setup 6 has the clamps on seven random sleepers loosened.
We can distinguish three frequency regimes. Between 200 an 400 Hz the mobility increases when more clamps are loosened. Between 400 Hz and 1000 Hz, the mobility decreases when the clamps are loosened. Starting at 1500 Hz, the typical range for rail dynamics, the clamps do not seem to play an important role as the mobility does not change. The frequency where the point mobility is reduced by loosening clamps is much lower than in the case of hard pads.
We would like to point out that Setup 6, having the clamps loosened on seven sleepers scattered over the length of the track, the effect on the mobility can be measured but it follows the curve of Setup 3 (clamps loosened on 3 consecutive sleepers).
In absolute numbers, the mobility power increases with a factor 5 at 200 Hz when the clamps of seven

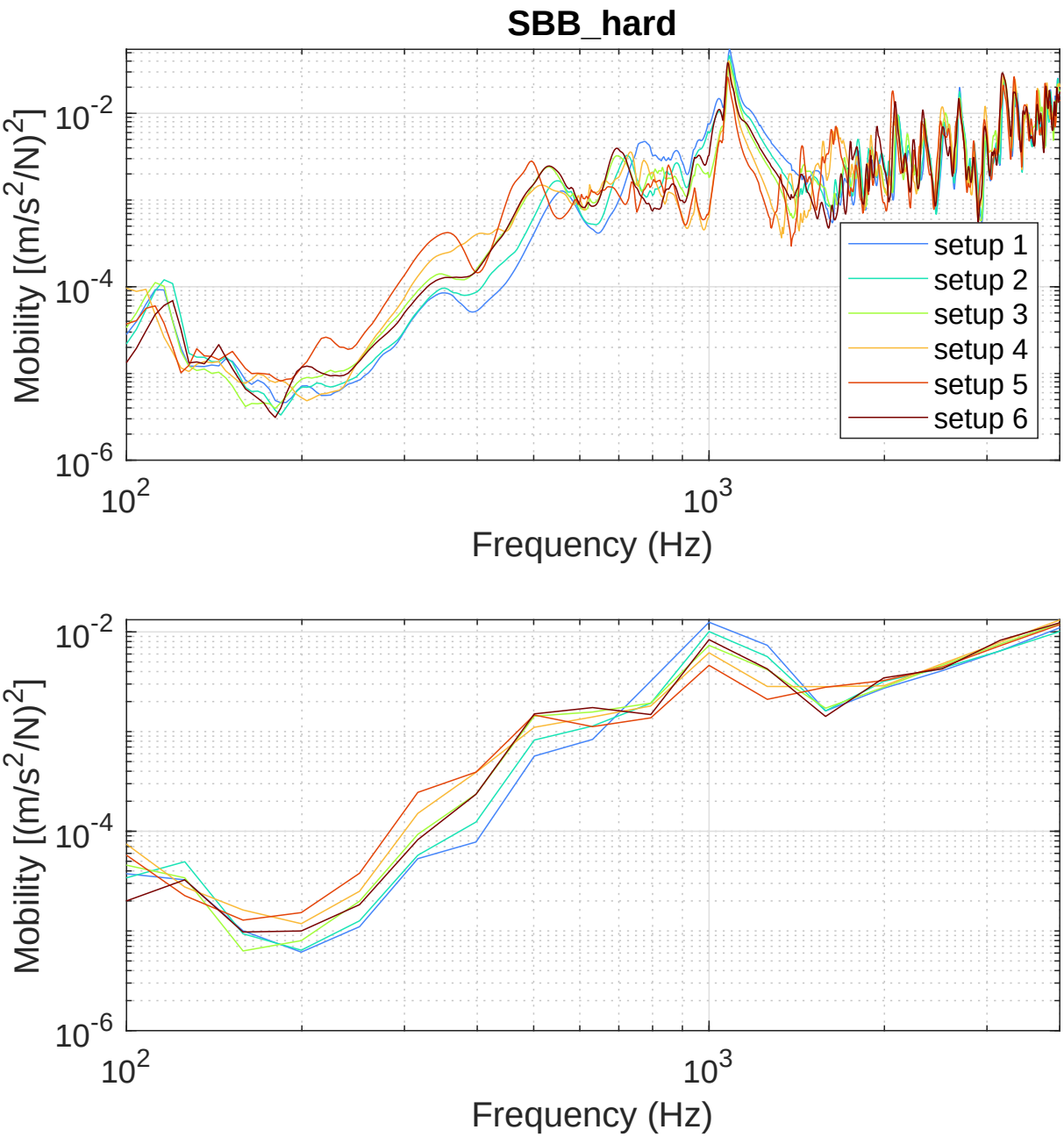

Figure 5: Point mobility of the test track with hard SBB pads.

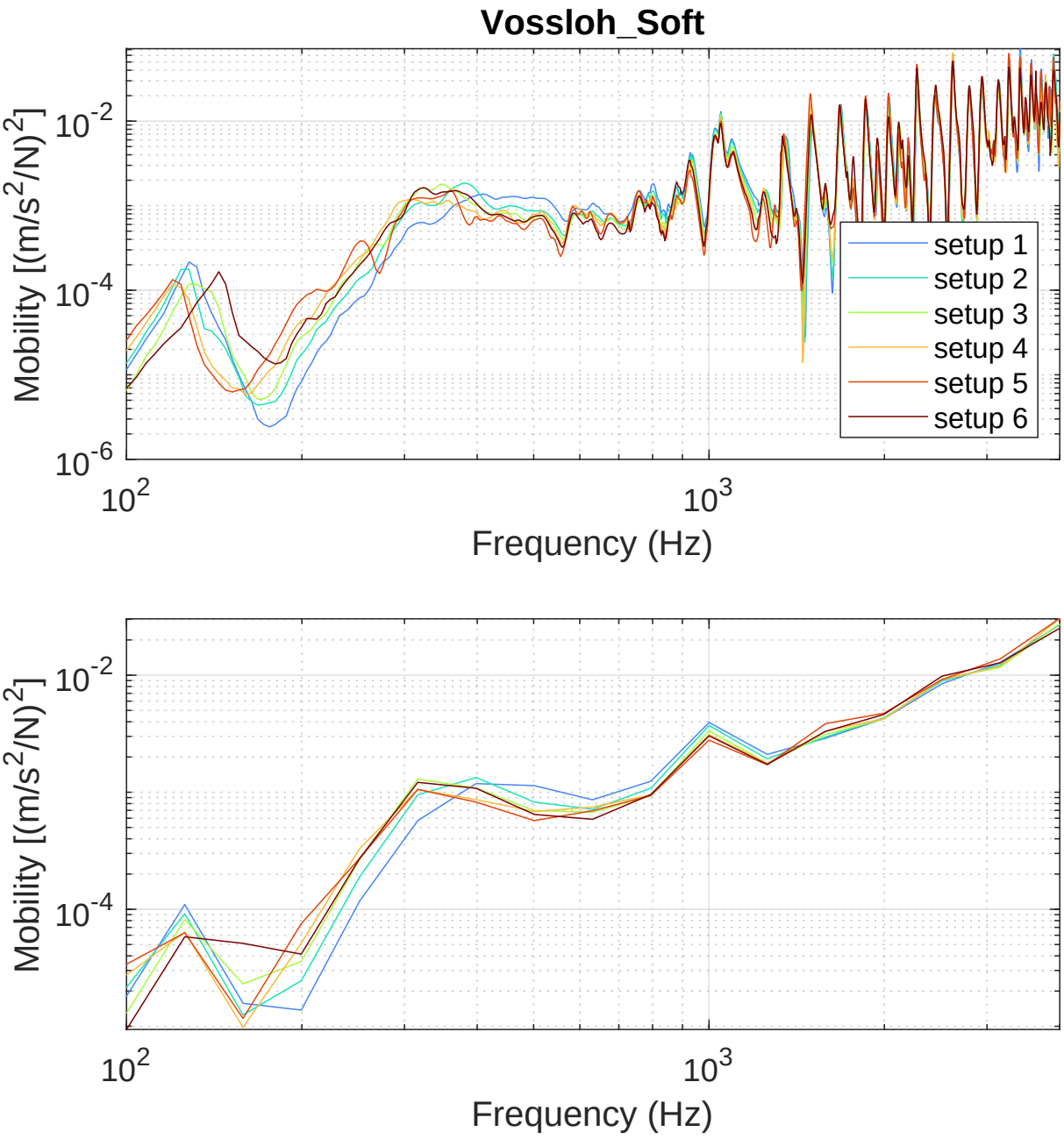

Figure 6: Point mobility of the test track with soft SBB pads.

consecutive sleepers are loosened. The mobility power is reduced by a factor 1.3 at the pin-pin frequency 1000 Hz in that case.

3.4 Damping Semperit pads

The mobility is shown in Fig. 7 for setup 1–6, 1 being all clamps tightened, and increasing the number of loose clamps up to setup 5. Setup 6 has the clamps on seven random sleepers loosened.
We can distinguish three frequency regimes. Between 200 an 800 Hz the mobility increases when more clamps are loosened. Between 900 Hz and 1500 Hz, the mobility decreases when the clamps are loosened. Starting at 1500 Hz, the typical range for rail dynamics, the clamps do not seem to play an important role as the mobility does not change. The frequency where the point mobility is reduced by loosening clamps is similar to the case of hard pads.
We would like to point out that Setup 6, having the clamps loosened on seven sleepers scattered over the length of the track, the effect on the mobility can be measured but it follows the curve of Setup 3 (clamps loosened on three consecutive sleepers).
In absolute numbers, the mobility power increases with a factor 2.5 at 400 Hz when the clamps of seven

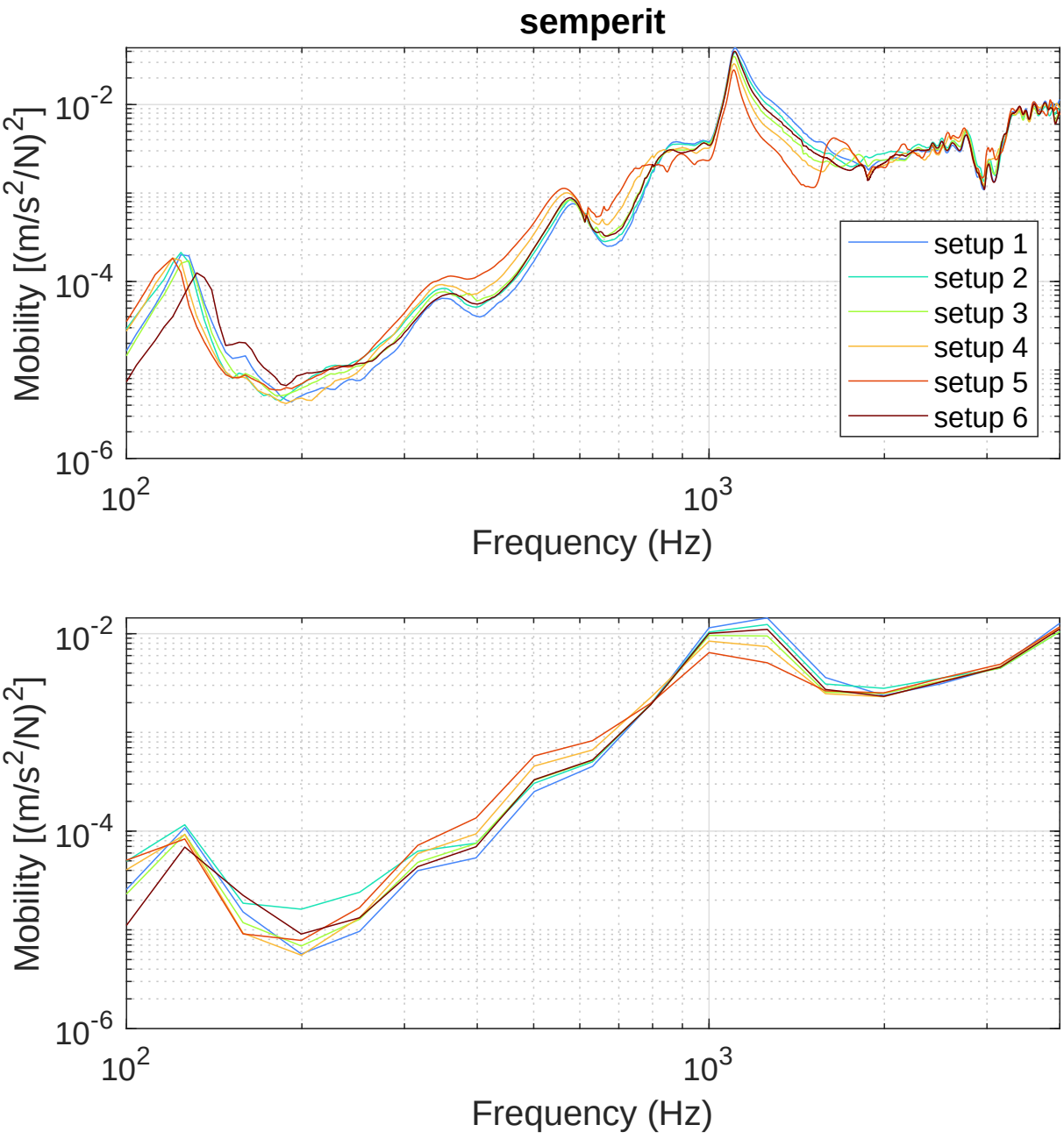

Figure 7: Point mobility of the test track with damping pads.

consecutive sleepers are loosened. The mobility power is reduced by a factor 2.8 at the 1250 Hz in that case.

3.5 Conclusion about point mobility

The point mobility changes differently depending on the frequency. In the range where the sleeper dynamics have effect (<800 Hz), the rail mobility increases when clamps are loosened. Around the first pin-pin frequency (1000 Hz), the rail mobility decreases when clamps are loosened. The effect at pin-pin is similar for all types of rail pads, the effect at low frequencies is smaller in case the pads are softer. From a physical point of view we can explain this behaviour as follows. At low frequencies the sleepers are not able to hold the rail by its clamps, therefore the rail becomes more mobile. The pin-pin frequency requires the presence of the clamps to create the standing wave with pins at the clamped points. If the clamps are not present, the boundary conditions for this mode are no longer present and it should eventually disappear. At even higher frequencies, the rail dynamics are less influenced by the clamps, and the pads mainly play the role of vibration dampers. However, for a small amount of loose clamps, the point mobility is not changing much. All clamps have to be loosened on at least five consecutive sleepers to see an important change of the mobility.

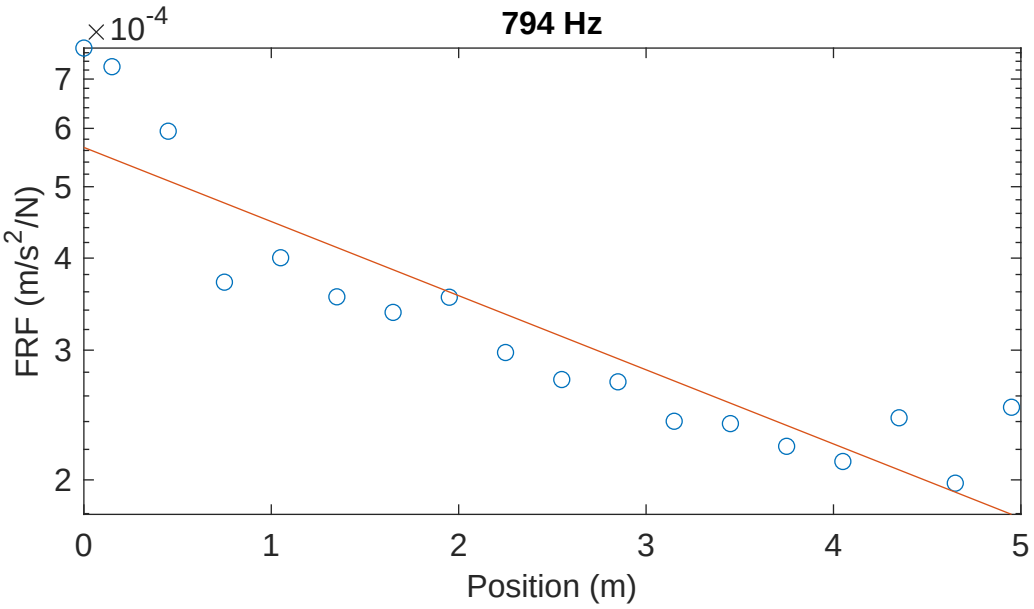

Figure 8: Example of the fitting to calculate the track decay rate at 794 Hz. Circles are measured FRF values, the red line is the best fit.

4 Track decay rate

4.1 Calculation of TDR

The track decay rate describes how fast a harmonic wave within a certain frequency band decays. The value is given in dB/m, thereby defining a fraction of the wave's energy disappearing per traveled meter of distance. According to the standard's theory, the content in every frequency band decays exponentially. Although this assumption is a simplification assuming that there is only one type of wave travelling, it allows for a universal and fairly reliable TDR calculation.
Since the length of the track does not allow for measurements far enough away from the source point (according to the standard, the response has to be measured up to the point where all frequency bands have decayed by 10 dB). We therefore calculate the TDR in a different way, by fitting the measured data $p(x)$ to a decaying exponential function $p(x) = p_0 \exp(-\beta x)$. The TDR is directly related to the decay constant: $TDR = -8.686\beta$. An example of the fitting is shown in Fig. 8.
Although this method is not perfect, because the measurement data include direct waves and reflected waves, it allows us to calculate a fairly reliable TDR based on near-field measurements.

4.2 SBB hard pads

The TDR is shown in the frequency range 200 - 4000 Hz in Fig. 9. We see a clear reduction of the TDR up to 2000 Hz when more clamps are loosened. However, unless the clamps of seven sleepers in a row are loosened, the TDR is still higher than the limit prescribed by Standard ISO 3095:2013. Above 2000 Hz, loosening clamps has little effect on the TDR value.
Quantitatively, the TDR decreases from 15 to 5.8 dB/m at its maximum value at 500 Hz.
Fig. 10 shows a comparison of the TDR measured on the test track and measured on a straight train track in Nottwil. The agreement is reasonable, showing the same trend over the entire frequency range. Differences are due to slightly different components (clamp and sleeper), different tightening of the clamps, the different calculation method, and mainly the absence of reflected waves in the infinitely long track.

4.3 SBB soft pads

The TDR is shown in the frequency range 200 - 4000 Hz in Fig. 11. We do not see a clear reduction of the TDR when more clamps are loosened. Moreover, in the frequency range between 400 and 800 Hz, the TDR is lower than the limit prescribed by Standard ISO 3095:2013.

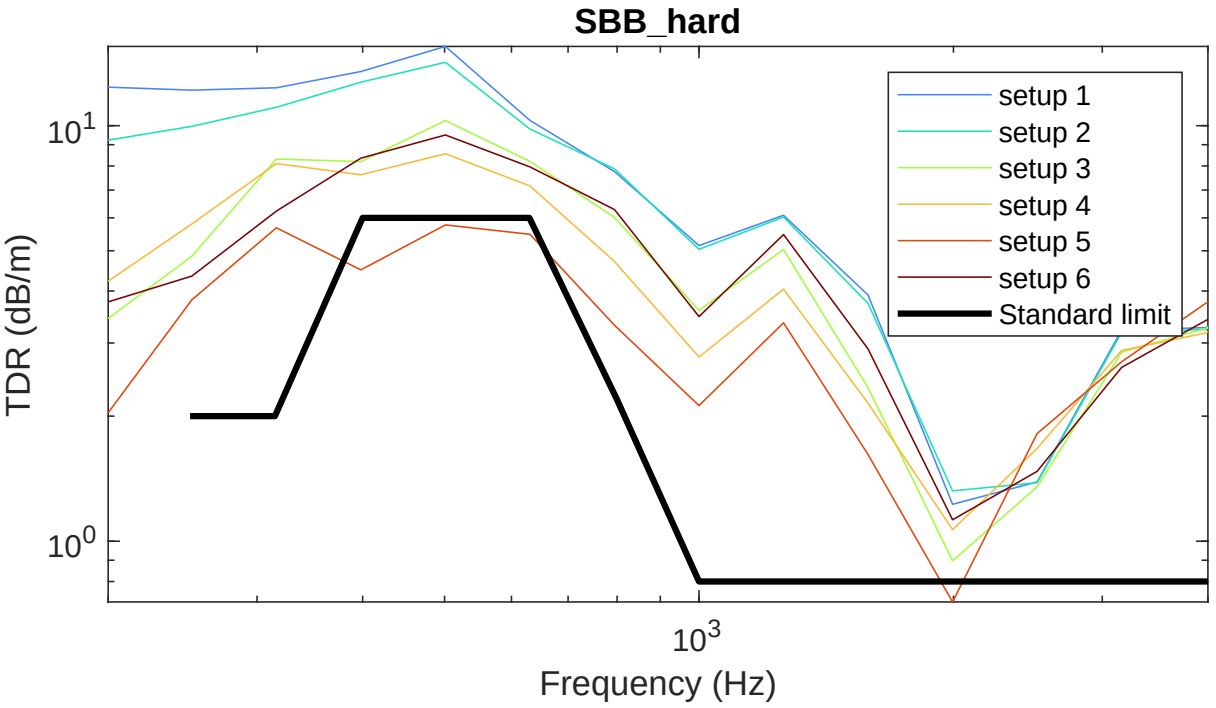

Figure 9: Measured TDR on the test track using hard SBB pads. The thick black line shows the lower limit defined in ISO 3095:2013.

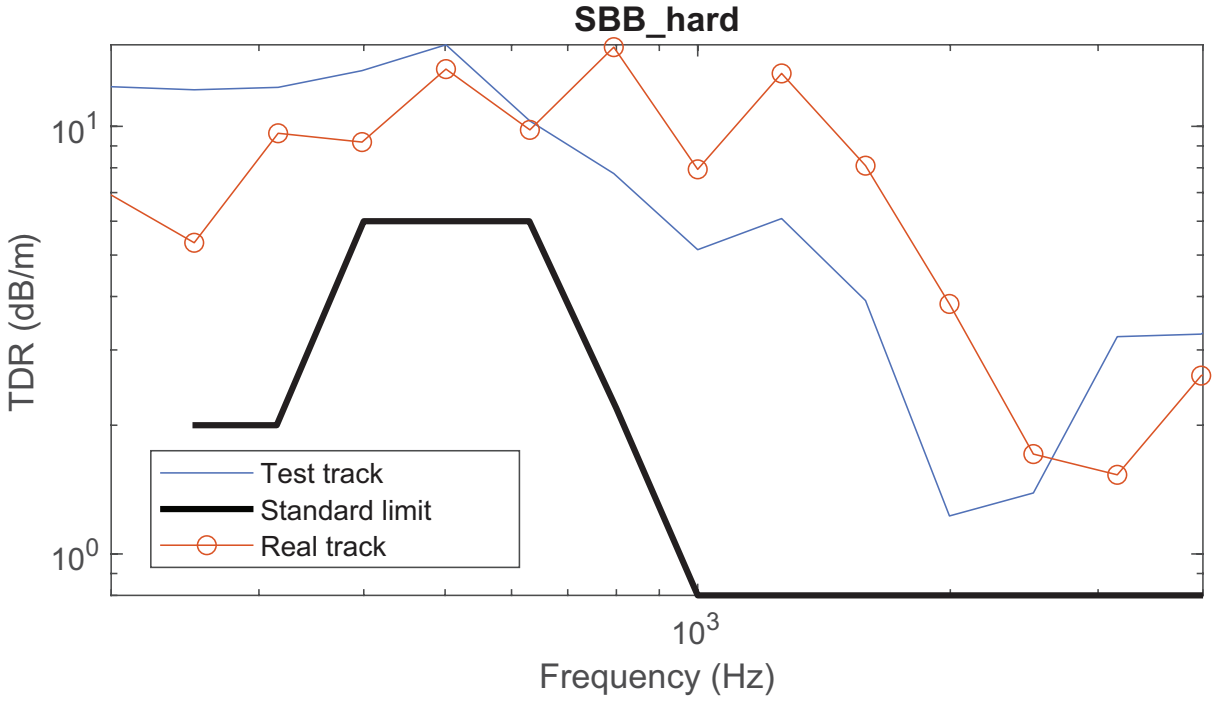

Figure 10: Measured TDR on the test track using hard SBB pads compared to the TDR measured on a real straight track section with the same pads. The thick black line shows the lower limit defined in ISO 3095:2013.

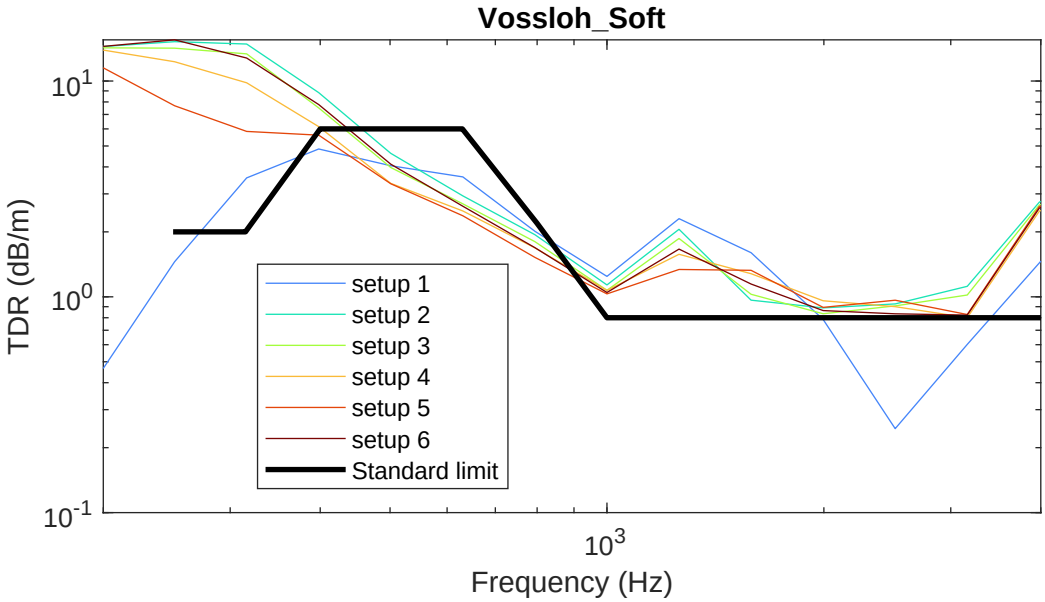

Figure 11: Measured TDR on the test track using soft SBB pads. The thick black line shows the lower limit defined in ISO 3095:2013.

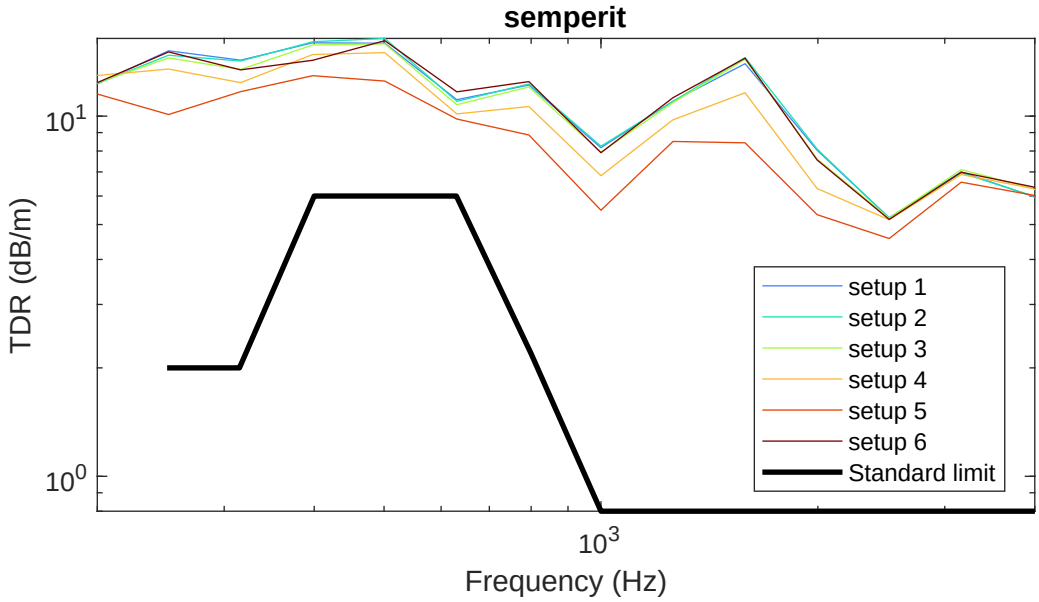

Figure 12: Measured TDR on the test track using damping pads. The thick black line shows the lower limit defined in ISO 3095:2013.

4.4 Damping Semperit pads

The TDR is shown in the frequency range 200 - 4000 Hz in Fig. 12. We see a clear reduction of the TDR up to 2000 Hz when more clamps are loosened. However, unless the clamps of sleepers in a row are loosened, the TDR is still higher than the limit prescribed by Standard ISO 3095:2013. Above 2000 Hz, loosening clamps has little effect on the TDR value.
Quantitatively, the TDR decreases from 16 to 12 dB/m at its maximum value at 500 Hz.
Fig. 13 shows a comparison of the TDR measured on the test track and measured on a straight train track in Nottwil. The agreement is reasonable, showing the same trend over the entire frequency range. Differences are due to slightly different components (clamp and sleeper), different tightening of the clamps, the different calculation method, and mainly the absence of reflected waves in the infinitely long track.

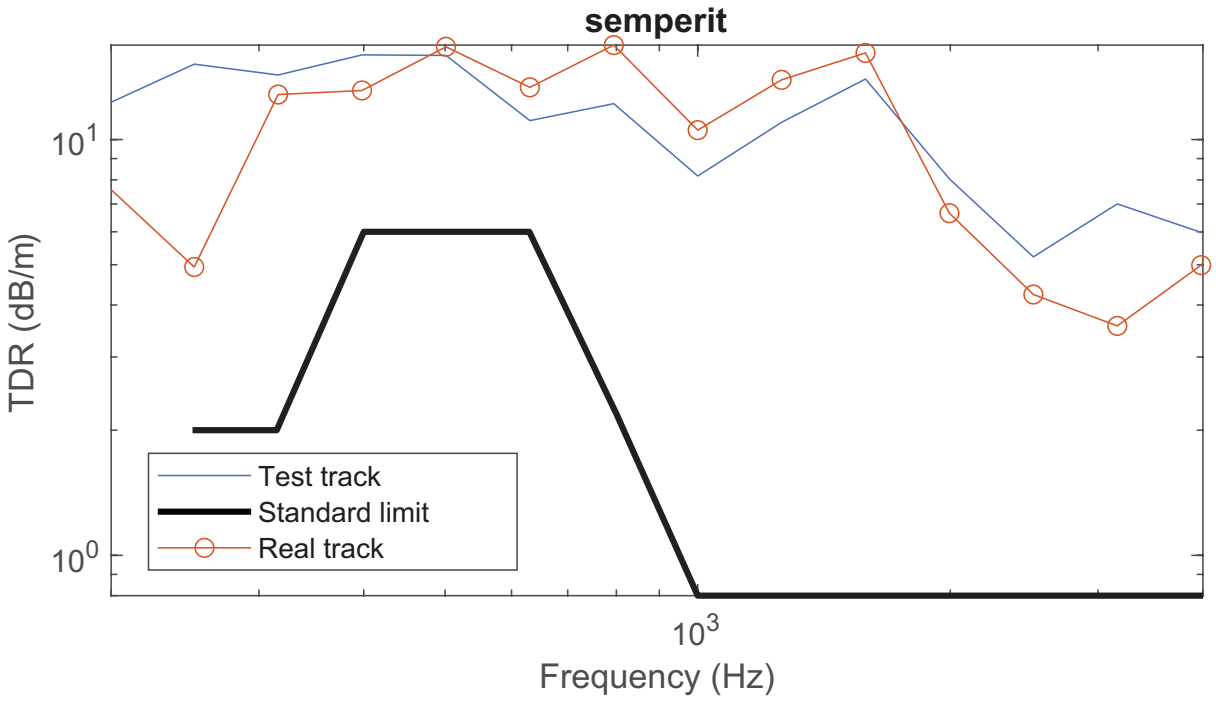

Figure 13: Measured TDR on the test track using damping pads compared to the TDR measured on a real straight track section with the same pads. The thick black line shows the lower limit defined in ISO 3095:2013.

4.5 Conclusion about TDR

Similar to the point mobility, we see a measurable change in TDR, given that the rail pads are not too soft. In the case of extremely soft PU rail pads, the rail is so much decoupled from the sleepers that loosening the clamps does not seem to have an effect on wave propagation.
Rail pads with higher damping and lower stiffness seem to have an overall better performance than hard pads. They reach higher TDR values, and are less sensitive to individual clamp errors.

5 Vibration transmission

5.1 Calculation of vibration transmission

We calculate the transfer function between the measured geophone signal and the rail acceleration at the location of the force input. The power spectra in third octave bands are calculated using the function `poctave` in Matlab R2020b. The transfer functions are then derived by taking the ratio of both power spectra.
Geophone measurements are very sensitive to external noise sources (ground vibrations from other sources than the excitation signal). The measurement was repeated ten times at each position and then averaged. To estimate the variability of the results, we took into account the measurements of all eight microphone positions as described in Section 2.6. In theory, since the track does not change for these measurements, all transfer function should be identical. The reported transfer functions are the average over the eight measurements. The experimental variability due to external noise is calculate als the standard deviation over these eight measurements.

5.2 SBB hard pads

The energy transmission using hard SBB pads is shown in Fig. 14. The largest difference can be seen at very low frequencies ($<$ 150 Hz). When loosening clamps, less energy is transmitted to the subgrade. A similar effect can be seen around 400 Hz, a typical vibration frequency of the sleeper.
The standard deviation over eight measurements of the three extreme setups is shown in Fig. 15. At low frequencies, there is a fairly large uncertainty for the individual measurements. However, between setup 1 and setup 5, the difference in transfer functions seems to be significant. Tightening the bolts again by hand (setup 7) does not seem to fully restore the results of setup 1, when an electrical wrench was used. The transmission remains lower at very low frequencies ($<$ 80 Hz).

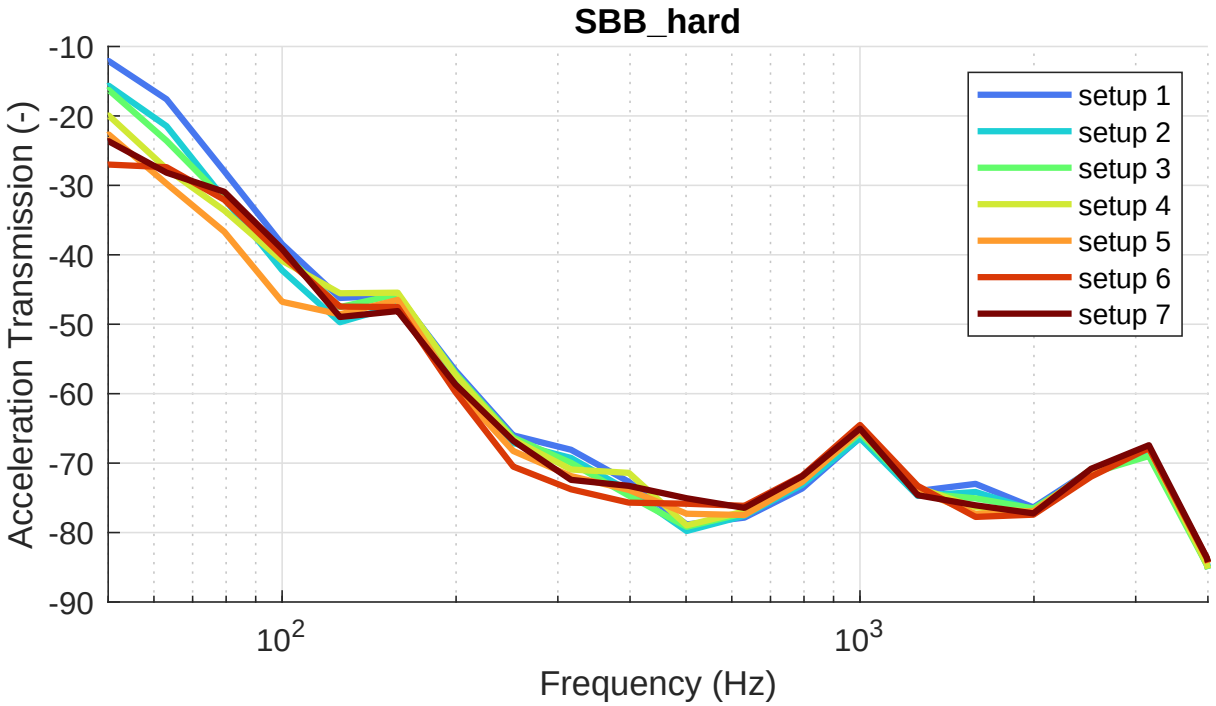

Figure 14: Measured energy transmission function from rail to subgrade for the 7 experimental setups using hard SBB pads.

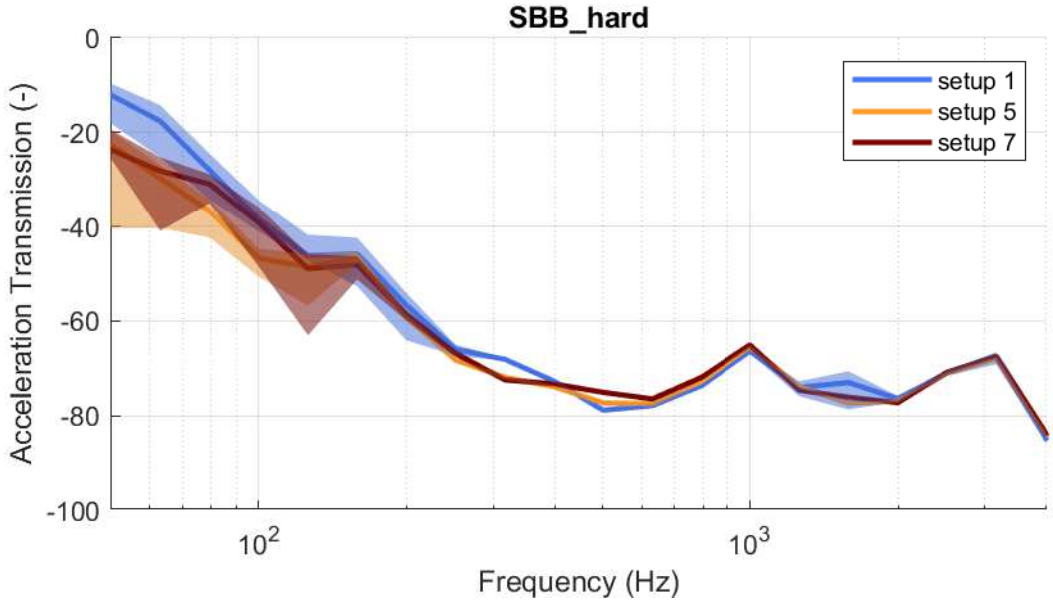

Figure 15: Measured energy transmission function from rail to subgrade for the three extreme experimental setups (all clamps fastened, setup 1 and 7, and all clamps loose, setup 5) using hard SBB pads.

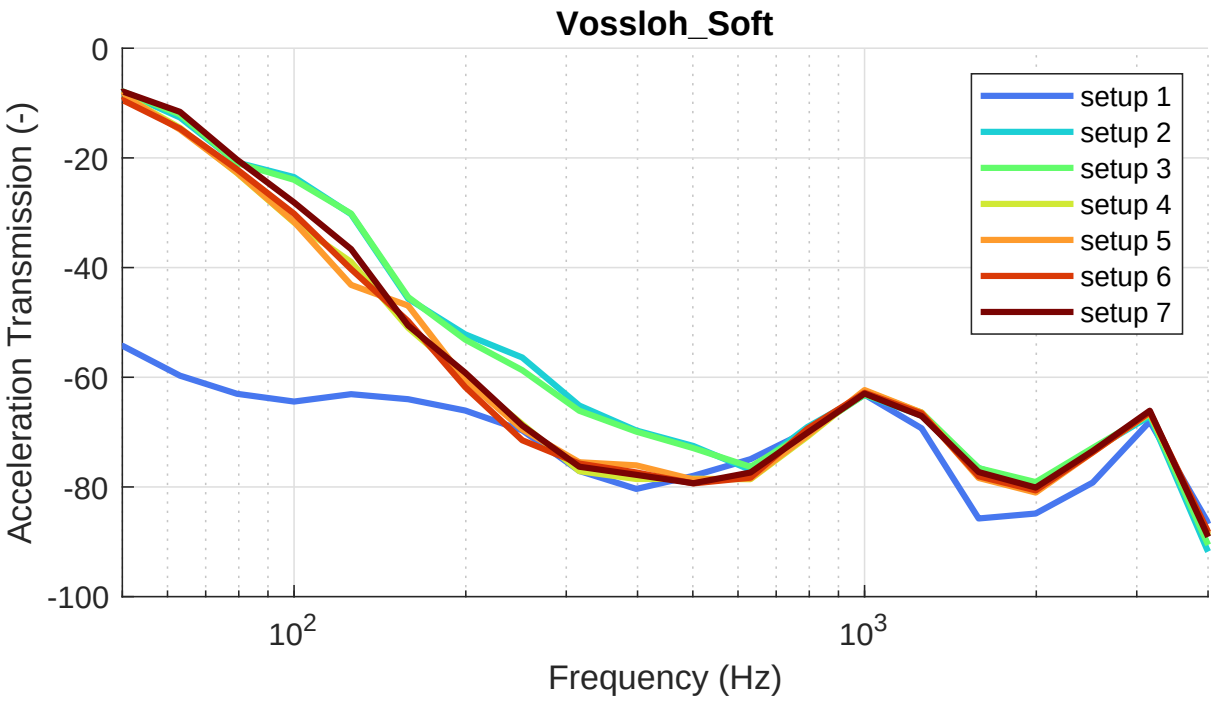

Figure 16: Measured energy transmission function from rail to subgrade for the 7 experimental setups using soft SBB pads.

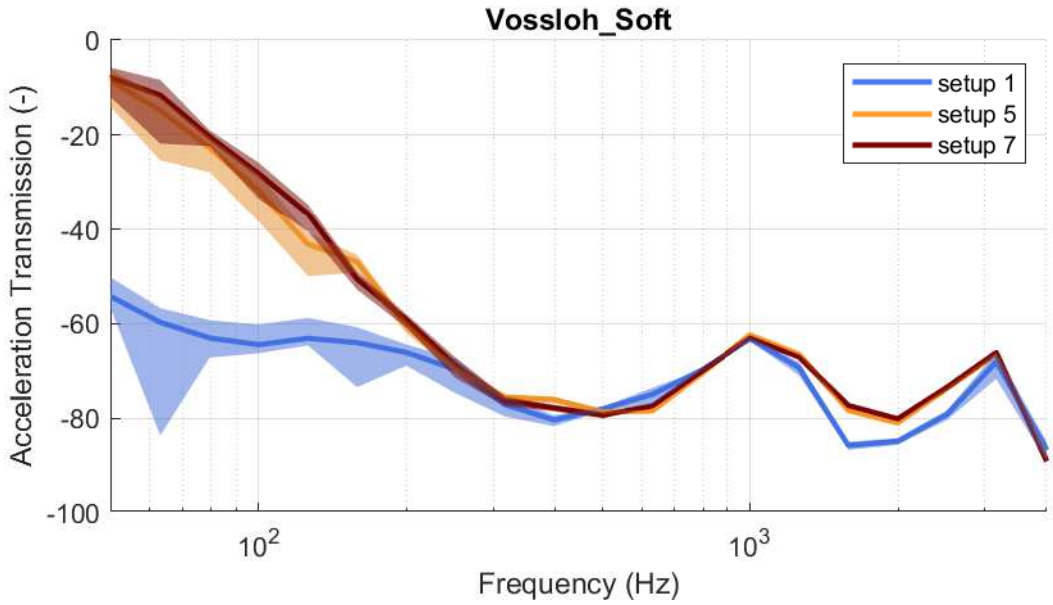

Figure 17: Measured energy transmission function from rail to subgrade for the three extreme experimental setups (all clamps fastened, setup 1 and 7, and all clamps loose, setup 5) using soft SBB pads.

5.3 SBB soft pads

Measuring the energy transmission using soft SBB pads, shown in Fig. 16, was not successful. Due to the soft pads and the high mobility of the rail, the shaker was detached from the rail at setup 1. This explains the low transmission in this case. We assume that experimental problems are also the reason for the high transmission in setups 2 and 3.

The measurements using setups 4–7 on the other hand are very consistent, both in average and standard deviation. This leads us to suspect that loosening the clamps plays a minimal role in changing the vibration energy transmission when soft rail pads are used.

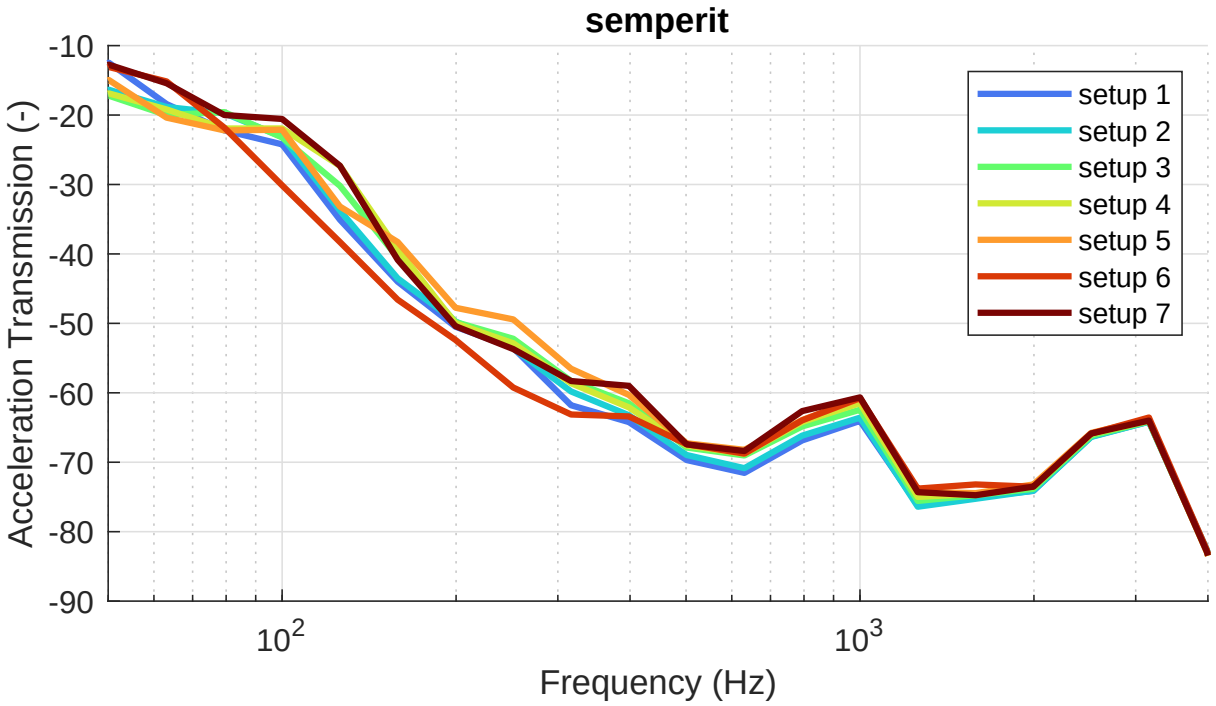

Figure 18: Measured energy transmission function from rail to subgrade for the seven experimental setups using damping pads.

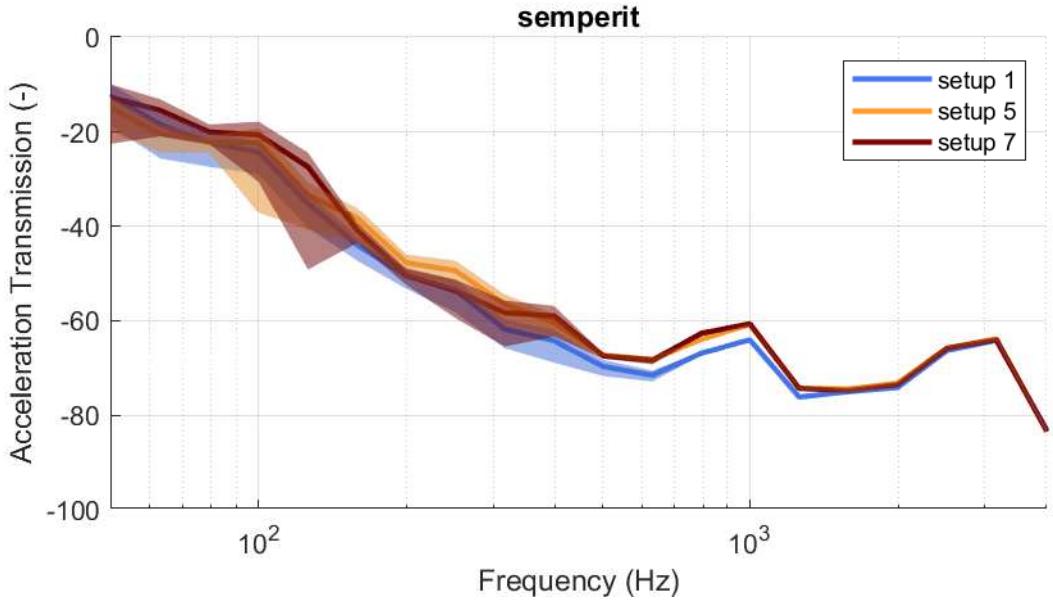

Figure 19: Measured energy transmission function from rail to subgrade for the three extreme experimental setups (all clamps fastened, setup 1 and 7, and all clamps loose, setup 5) using damping pads.

5.4 Damping Semperit pads

The energy transmission using damping pads is shown in Fig. 18. There is no clear trend at low frequencies, except for setup 6 (seven sleepers with loose clamps, scattered over the entire track), which seems to reduce the vibration transmission. For all other setups, the transmission lies between setup 1 and setup 7, both representing a totally fastened track.
The standard deviation over eight measurements of the three extreme setups is shown in Fig. 19. At low frequencies, the uncertainty is so large that no conclusions can be drawn.

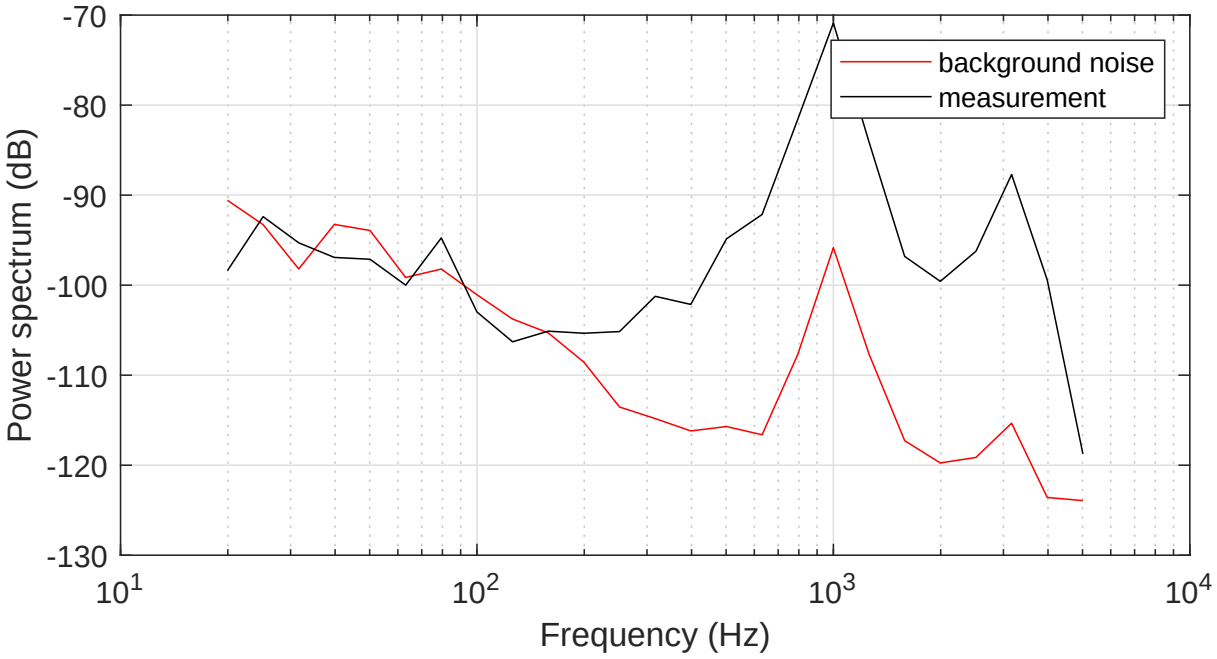

Figure 20: Background noise measurement in comparison to a measured signal when the rail is excited by the shaker using hard SBB pads.

5.5 Conclusion about energy transmission to the subgrade

Measuring vibration transmission through the ballast bed leads to similar trends for all rail pads. When all clamps are fastened, the transmission loss is around 15-20dB in the frequency range below 100 Hz. Between 100 and 700 Hz there is a fast reduction of transmitted energy to 70-80dB. Above 800 Hz, the transmitted energy remains at a very low level. This is in line with the common knowledge that ballast is a very efficient vibration isolator for all but the lowest frequencies.
Comparing the hard SBB pads and intermediate-stiffness Semperit pads, we can conclude that there is a significant reduction of vibration energy transfer using hard pads when clamps are loosened. This makes sense from a practical standpoint: the rails are decoupled from the sleepers, so that the sleepers move less and inject less energy into the ballast. Softer pads are already better decoupled from the sleepers, even if the clamps are fastened. Therefore, there is no discernible difference when the clamps are loosened.
As a final remark, we want to point out that the measurements at below 150 Hz are not substantially above the noise floor given the noisy environment with heavy construction work nearby. The power spectral density of the noise compared to the measurement is shown in Fig. 20. The peaks in the noise signal are due to internal resonances of the geophone, which can occur above 1000 Hz according to the sensor's data sheet.

6 Acoustic radiation

6.1 Calculation of the emitted sound power

The measurement closely follows the sound power method using a cylindrical measurement surface around the radiating rail (ISO 3745:2012, [3]). We scan the cylindrical surface using seven microphones 1 m away from the rail, while the array is moved in 0.1 m steps from one sleeper to the next. Although prescribed by the norm, we cannot do the test in a semi-anechoic room.
The A-weighted sound pressure energy spectrum L_{Pi} is calculated in third-octave bands for each microphone, leading to $N_m = 7 \times 7 = 49$ measurement points. The surface average sound pressure level is then calculated over all these points:

$$\bar{L_P'} = 10 \log \left(\frac{1}{N_m} \sum_{i=1}^{N_m} 10^{0.1 L_{Pi}} \right). \quad (1)$$

The sound power is finally given by $L_W = \bar{L_P'} + 10 \log(S/S_0)$, where S is the area of the measurement surface and $S_0 = 1$ m^2.
In addition, we also present the average sound pressure level in measurement position 0, close to sleeper 9 which is loosened for all setups except setup 1 and 7.

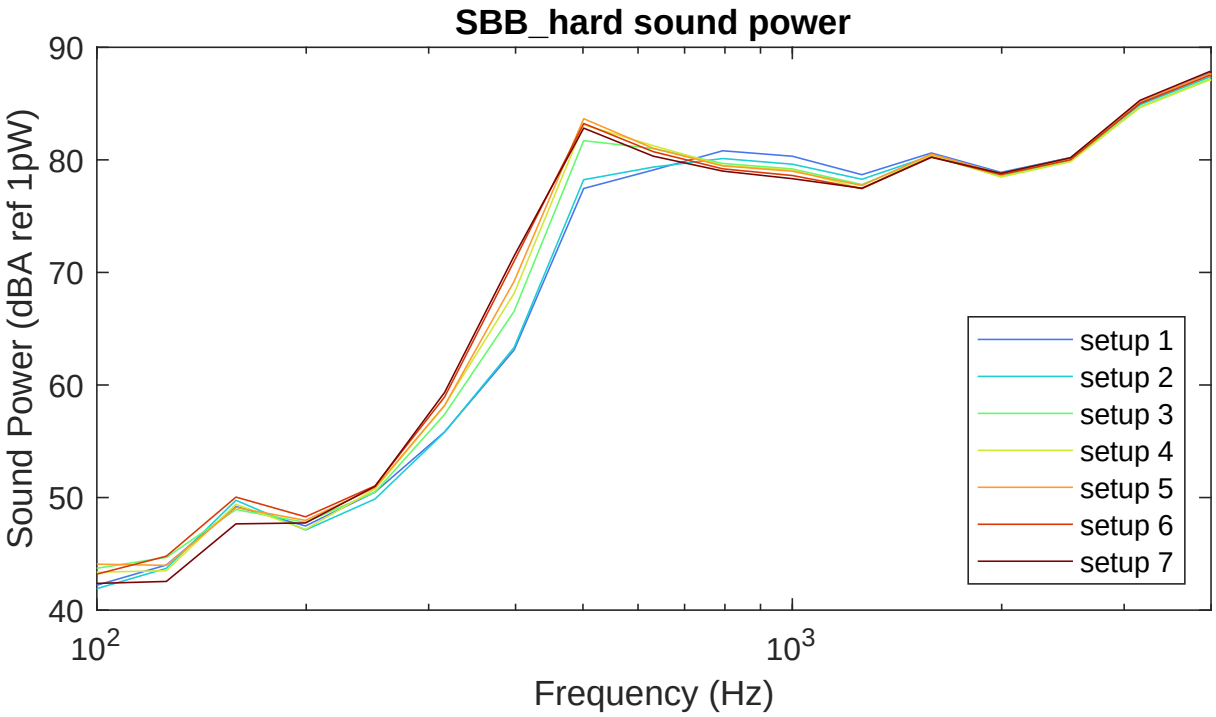

Figure 21: Radiated sound power level of the rail between sleeper 12 and 13 using hard SBB pads.

6.2 SBB hard pads

The measurements of the sound power (Fig. 21) show an increase in radiated noise in the 300-700 Hz range, which is consistent with the increased rail mobility. Around 1000 Hz, the noise radiation decreases slightly. Due to the A-weighting, the increased noise radiation is relatively low thanks to the lower perception in this frequency range. The only potential problematic frequency band is at 500 Hz, where a 6 dB increase can be noticed. The maximum noise decrease of 2 dB can be found at 1000 Hz.
It has to be remarked that the sound power curve for setup 7, tightening all bolts, does not return to the base curve at setup 1. Given the rainy conditions on the day of the measurement, it is possible that the measurements were influenced by noise from the weather. The time schedule unfortunately did not allow for additional measurements.
At measurement position 0, closer to the shaker and next to the loose sleeper 9, there seems to be a small increase in radiated sound between 1000 and 3000 Hz, despite the decreased mobility (Fig. 21) . However, since the TDR decreases significantly in this frequency range, this could also lead to higher noise levels.

6.3 SBB soft pads

The measurements of the sound power (Fig. 23) show no change radiated noise in the 300-700 Hz range, not taking setup 1 into account due to the faulty measurement where the shaker detached from the rail. At low frequencies the curves are slightly different, probably due to the low sound power levels at these frequencies and therefore larger measurement errors.
At measurement position 0, closer to the shaker and next to the loose sleeper 9, there seems to be a small increase in radiated sound between 1000 and 3000 Hz, despite the decreased mobility (Fig. 24). However, since the TDR decreases in this frequency range, this could also lead to higher noise levels.

6.4 Damping Semperit pads

The measurements of the sound power (Fig. 25) show almost no change in radiated sound power.
At measurement position 0, closer to the shaker and next to the loose sleeper 9, there seems to be a small increase in radiated sound between 1000 and 3000 Hz, despite the decreased mobility (Fig. 25). However, since the TDR decreases in this frequency range, this could also lead to higher noise levels.

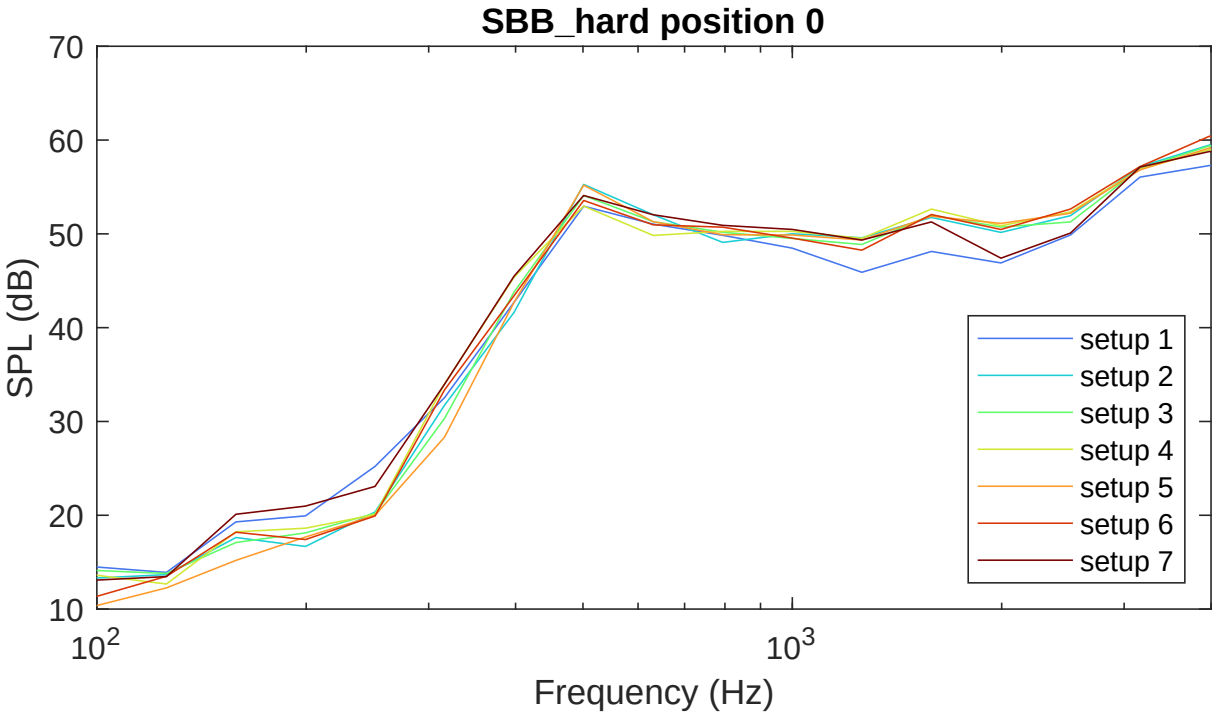

Figure 22: Radiated sound pressure level of the rail between sleeper 9 and 10 using hard SBB pads.

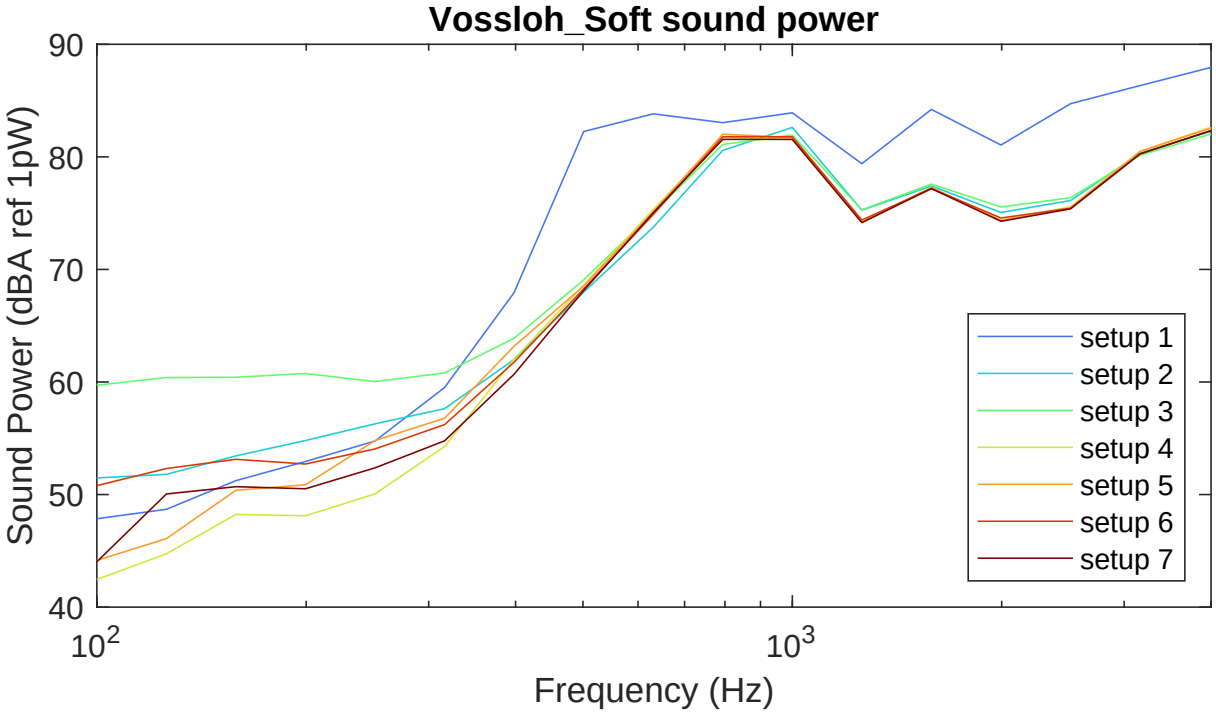

Figure 23: Radiated sound power level of the rail between sleeper 12 and 13 using soft SBB pads.

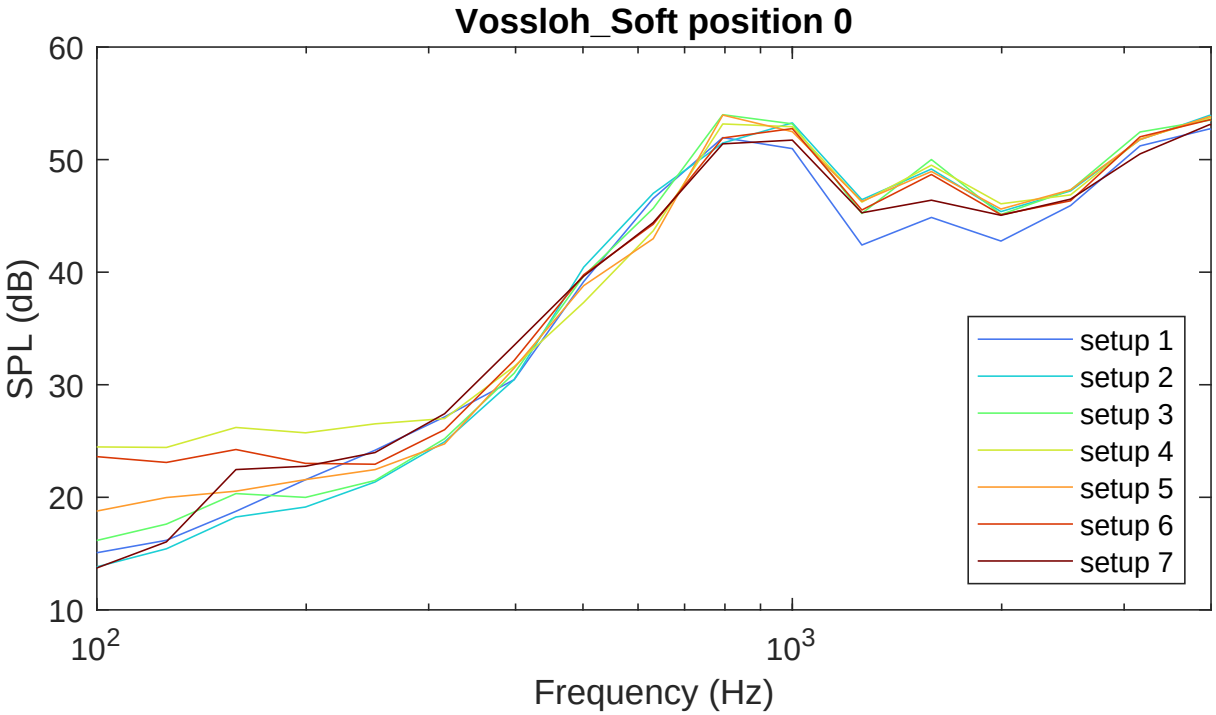

Figure 24: Radiated sound pressure level of the rail between sleeper 9 and 10 using soft SBB pads.

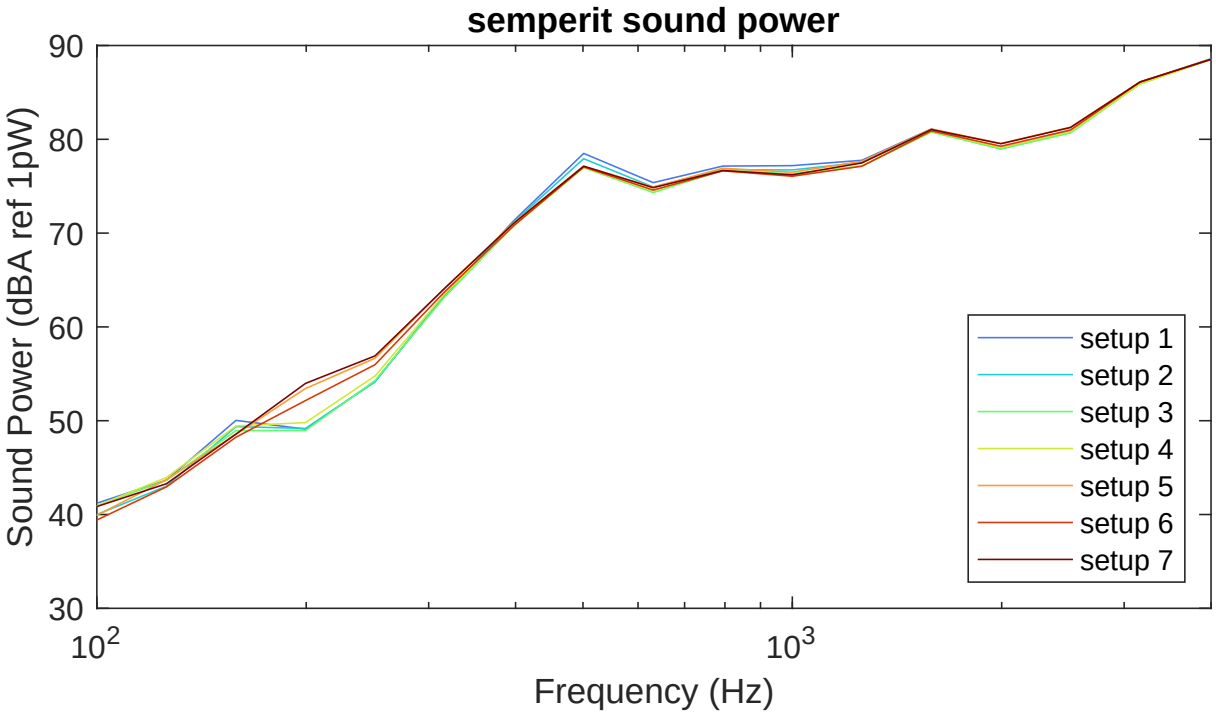

Figure 25: Radiated sound power level of the rail between sleeper 12 and 13 using damping pads.

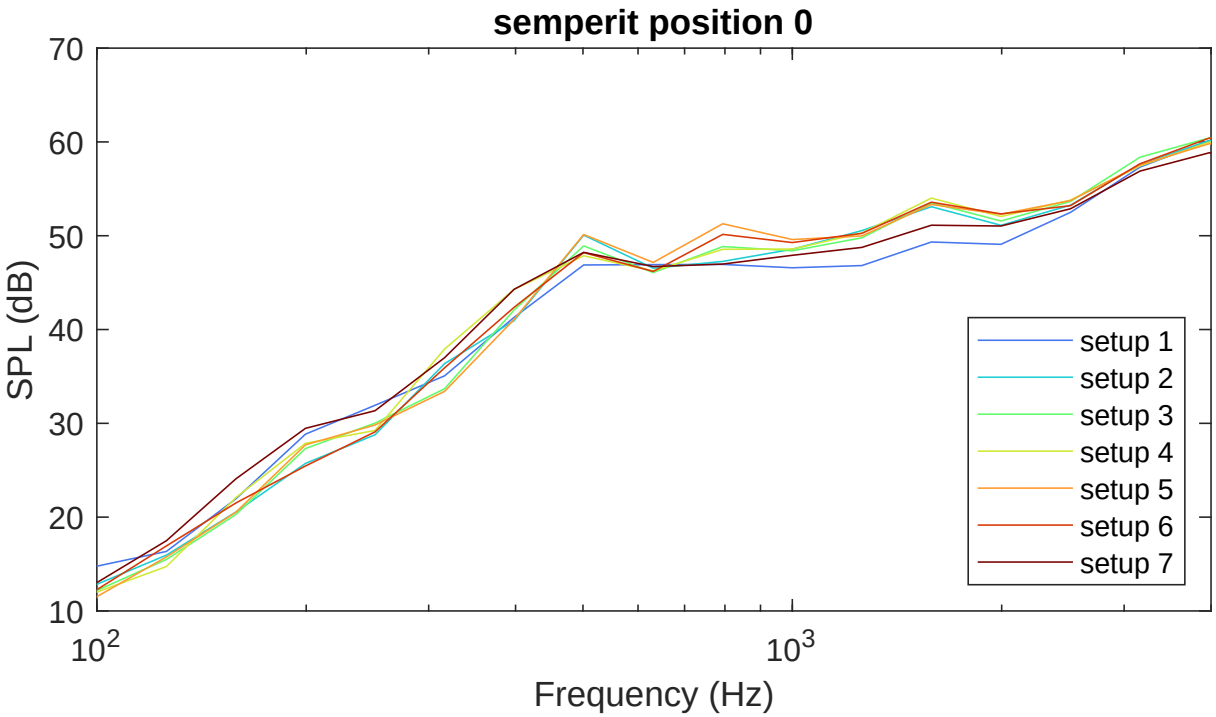

Figure 26: Radiated sound pressure level of the rail between sleeper 9 and 10 using damping pads.

6.5 Conclusion about acoustic radiation

Sound power measurements between sleeper 12 and 13 show minor changes in the radiated sound power level for soft and intermediate rail pads, despite measurable differences in the rail mobility and TDR. The microphone capture however a combination of radiated noise from the rail, the sleepers, and the shaker. It is possible that the reduced sleeper vibration cancels out the increased rail vibration.
The hard SBB pads seem to lead to slightly higher noise radiation below 800 Hz, although it cannot be excluded that the reason for this is increased background noise due to the rainy weather.
Closer to the shaker, there seems to be a slightly higher sound pressure level in the 1000-3000 Hz range. The reason for this could be the decrease in TDR, which leads to higher rail vibration levels in the vicinity of the shaker.
Fig. 27 finally shows the background noise level of a microphone compared to a typical measurement using, averaged over the seven microphones of the array. Starting at 400 Hz, the signal-to-noise ratio is higher than 10 dB, meaning that the results should be reliable in that range.

7 Overall conclusion

We have measured the dynamic response of a test track using three different rail pads, increasing the number of loosened rail clamps. The rail dynamics, which can be measured with very low noise levels, show clear trends. The point mobility increases at frequencies governed by the sleeper vibrations, and decreases around the pin-pin resonance frequency. The TDR decreases when more clamps are loose. However, the presence of a small number (up to three sleepers) of loose clamps only leads to minor changes. The effects become smaller when the rail pads are softer, since the rail is more decoupled from the sleepers even when the clamps are properly tightened.
The comparative measurements on the test track show that well-designed rail pads with higher viscoelastic damping reduce the rail mobility and TDR in the acoustically relevant range from 500 Hz, compared to standard hard and soft pads. Due to their lower stiffness, the clamping system has less influence on the dynamic behaviour of the rails than for hard SBB pads.
Vibration transmission results are inconclusive, since the noise levels were too high to allow quantitative analyses of the data. In the frequency range above 300 Hz, loosening the clamps does not seem to have an effect on the transmitted vibration energy.
The acoustic radiation does not seem to change measurably in the higher frequency range >800 Hz and far enough away from the excitation source. Only if hard pads are used, the radiated sound power seems to correlate with the increased rail mobility at lower frequencies, although the background noise also increased

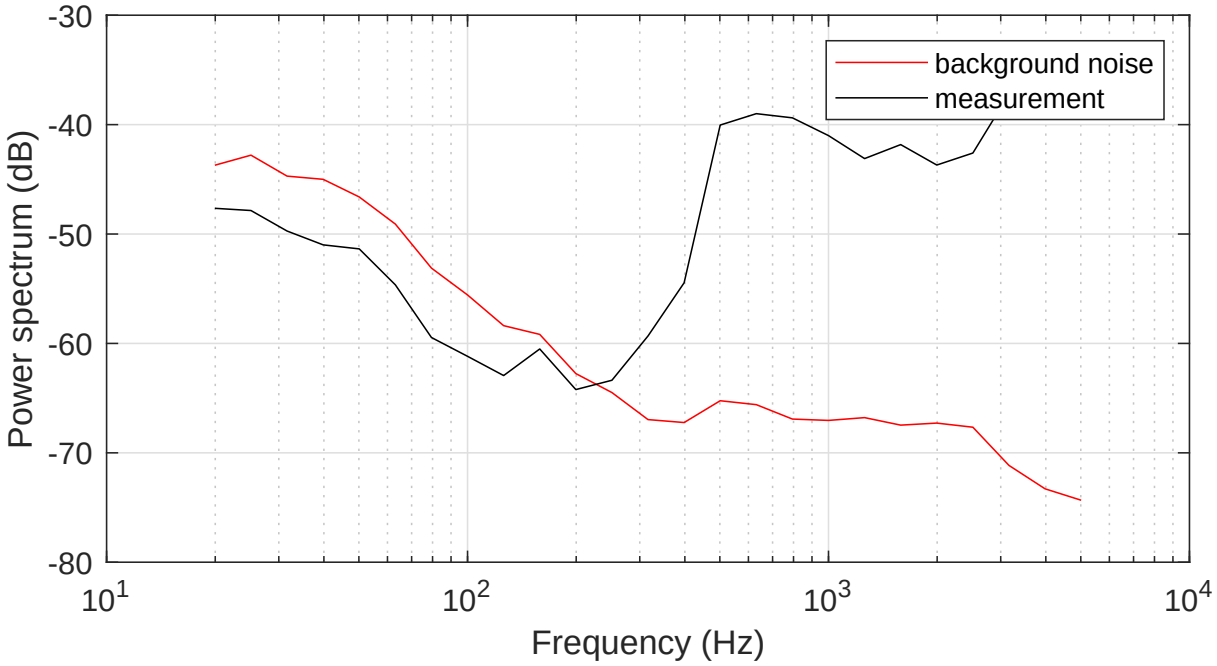

Figure 27: Comparison of the microphone background noise level compared to a measurement signal using hard SBB pads.

due to rain. Closer to the excitation source, there is an increase of sound power in the 1000-3000 Hz range. This can be explained by the reduced TDR.
Overall, we see only small changes in perceptible effects (noise and vibration exposure), even in the extreme case where the clamps of 7 sleepers in a row are loosened. From this preliminary study, we would conclude that up to 15% loose clamps do not lead to important higher noise or vibration levels. Moreover, we expect that the effects during pass-by, where the weight of the train confines the rails in addition to the clamps, should be even smaller. This would require tests on a track in use (insofar safety can be ensured) or extensive modelling.
Models of the effect of loose clamps could include changing the stiffness of the rail-sleeper contact in analytical models. However, a change of stiffness only might be too simplistic to capture more complex effects, such as the detaching of the rail from the sleeper when it moves upward. In this case, the detailed behaviour of the combination of a rail pad and a loose clamp must be measured first.

References

[1] Kompetenzzentrum Fahrbahn, Forschungsprojekt Schienenbefestigung Phase I Schlussbericht, 2021.

[2] HEIG, Study of rail clamps preload influence on ballast solicitation and acoustic emissions, 2021.

[3] ISO 3745:2012, Akustik - Bestimmung der Schallleistungs- und Schallenergiepegel von Geräuschquellen aus Schalldruckmessungen - Verfahren der Genauigkeitsklasse 1 für reflexionsarme Räume und Halbräume

[4] Haladin, I., Lakusic, S. and Koscak, J., 2016. Measuring vibration damping level on conventional rail track structures. Diesel locomotives, 84, p.99.